Simulation of 6DOF motion control loop of three-channel flight device

Nguyen Van Khoi*, To Ba Thanh, Bui Van Tuan

Academy of Military Science and Technology, 17 Hoang Sam, Cau Giay, Hanoi, Vietnam.
*Corresponding author: vankhoi2603@gmail.com
Received 03 Nov. 2024; Revised 16 Dec. 2024; Accepted 25 Dec. 2024; Published 25 Feb. 2025.
DOI: https://doi.org/10.54939/1859-1043.j.mst.101.2025.3-12

ABSTRACT

The article presents a method for constructing a control system and simulating the closed-loop control of a 6-degree-of-freedom (6DOF) motion for a three-channel flight device (TLCT-3), modeled after the Javelin. Based on publicly available data on the tactical and technical features of the TLCT-3, the authors analyzed and calculated the geometric, inertial, and aerodynamic characteristics to provide input data for the controlled object in the simulation program. At the same time, the research team developed models for the command generation block, autopilot block, and controlled object block to design the simulation program. The simulation results, based on two scenarios of top attack and direct attack modes, confirm the accuracy of the models and their alignment with the tactical and technical features of the TLCT-3.

Keywords: Three-channel flight device; Control loop simulation; 6DOF motion.

1. INTRODUCTION

The three-channel flight device modeled after the Javelin (TLCT-3) is a critical weapon that has proven effectively in numerous engagements. With advancements in science and technology, TLCT-3 systems are increasingly modernized, enhancing their features and effectiveness [1, 2]. Although the TLCT-3 has been deployed, publicly available information is primarily limited to its tactical and technical specifications due to technology confidential requirements. Existing studies mainly focus on the TLCT-3 control system in general, without delving into the details of the Javelin variant or addressing the entire control mission of the system.

For the task of modeling the TLCT-3 control system, several studies have focused on the command generation block [3, 4]. These studies primarily aim to improve guidance laws based on kinematic models and constraints related to the seeker's field of view and target approach angles. However, most of these works address the problem in a single plane and do not consider the inertial characteristics and cross-channel coupling of the controlled object. Notable in this field is the study by Harris et al. [5], which developed a 6DOF flight dynamics model, a control system model, and a simulation of top attack scenarios. However, the TLCT-3-specific data used in this study only included basic components, without considering cross-channel coupling. Moreover, the autopilot block was not clearly described, and the command generation block lacked integration of a direct attack mode, which would enable effective engagement of targets at close range.

In this article, the authors focus on developing a control system model for the TLCT-3 with two main components: the command generation block and the autopilot block. The model is designed to close the control loop, supporting both tactical scenarios: top attack and direct attack, while fully integrating the characteristic data of the TLCT-3.

2. PROBLEM

2.1. Dynamic model of the three-channel flight device

The dynamic model of the three-channel flight device modeled after the Javelin (TLCT-3) is constructed within the ground coordinate system $x_Ey_Ez_E$, the body coordinate system $x_By_Bz_B$, and the non-rotating coordinate system $x_{NR}y_{NR}z_{NR}$. The flight dynamics model of the TLCT-3 includes the following components [5]:

1) The translational motion of the center of mass in the body coordinate system $x_By_Bz_B$:

$$\begin{bmatrix}\dot{u}\\ \dot{v}\\ \dot{w}\end{bmatrix}=\frac{1}{m}\begin{bmatrix}X\\ Y\\ Z\end{bmatrix}-\begin{bmatrix}0 & -r & q\\ r & 0 & -p\\ -q & p & 0\end{bmatrix}\begin{bmatrix}u\\ v\\ w\end{bmatrix} \quad (1)$$

Where *[u, v, w], [X, Y, Z]* and *[p, q, r]* are the components of velocity, external force, and angular velocity, respectively, in the $x_By_Bz_B$ coordinate system, and m is the mass of the TLCT-3.

2) The rotational motion around the center of mass in the body coordinate system $x_By_Bz_B$:

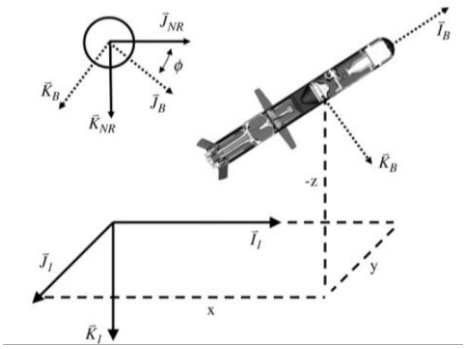

Figure 1. *Reference coordinate systems.*

$$\begin{bmatrix}\dot{p}\\ \dot{q}\\ \dot{r}\end{bmatrix}=\begin{bmatrix}1/I_{xx} & 0 & 0\\ 0 & 1/I_{yy} & 0\\ 0 & 0 & 1/I_{zz}\end{bmatrix}\left(\begin{bmatrix}L\\ M\\ N\end{bmatrix}-\begin{bmatrix}0 & -r & q\\ r & 0 & -p\\ -q & p & 0\end{bmatrix}\begin{bmatrix}I_{xx} & 0 & 0\\ 0 & I_{yy} & 0\\ 0 & 0 & I_{zz}\end{bmatrix}\begin{bmatrix}p\\ q\\ r\end{bmatrix}\right) \quad (2)$$

Where *[L, M, N]* are the components of the external moment forces, and *[I_{xx}, I_{yy}, I_{zz}]* are the components of the moments of inertia.

3) Translational motion of the center of mass in the ground coordinate system $x_Ey_Ez_E$:

$$\begin{bmatrix}\dot{x} & \dot{y} & \dot{z}\end{bmatrix}^T=C_b^n\begin{bmatrix}u & v & w\end{bmatrix}^T \quad (3)$$

4) Rotational motion around the center of mass in the ground coordinate system $x_Ey_Ez_E$:

$$\begin{bmatrix}\dot{\phi}\\ \dot{\theta}\\ \dot{\psi}\end{bmatrix}=\begin{bmatrix}1 & \sin\phi\tan\theta & \cos\phi\tan\theta\\ 0 & \cos\phi & -\sin\phi\\ 0 & \sin\phi/\cos\theta & \cos\phi/\cos\theta\end{bmatrix}\cdot\begin{bmatrix}p\\ q\\ r\end{bmatrix} \quad (4)$$

The total external forces acting on the TLCT-3 include gravitational force ($\boldsymbol{F}_G$), aerodynamic forces acting on the body and lifting wings ($\boldsymbol{F}_A$), control aerodynamic forces acting on the control fins ($\boldsymbol{F}_F$), and thrust vector control (TVC) forces ($\boldsymbol{F}_{TVC}$).

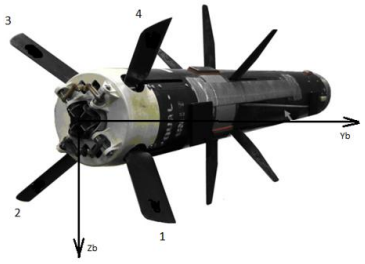

Figure 2. *Aerodynamic configuration of TLCT-3.*

$$\begin{bmatrix}X\\ Y\\ Z\end{bmatrix}=\begin{bmatrix}X_G\\ Y_G\\ Z_G\end{bmatrix}+\begin{bmatrix}X_A\\ Y_A\\ Z_A\end{bmatrix}+\begin{bmatrix}X_F\\ Y_F\\ Z_F\end{bmatrix}+\begin{bmatrix}X_{TVC}\\ Y_{TVC}\\ Z_{TVC}\end{bmatrix} \quad (5)$$

Where the external force components are determined as follows:

$$\begin{bmatrix}X_G\\ Y_G\\ Z_G\end{bmatrix}=C_n^b\begin{bmatrix}0\\ 0\\ mg\end{bmatrix};\quad \begin{bmatrix}X_A\\ Y_A\\ Z_A\end{bmatrix}=\begin{bmatrix}-CA(M,\alpha_s,p,q,r)\\ CY(M,\beta,p,r)\\ CN(M,\alpha,\dot{\alpha},q)\end{bmatrix}q_{din}S\approx\begin{bmatrix}-CA(M,\alpha_s)\\ CYB(M)\beta+CYP(M)\bar{p}+CYR(M)\bar{r}\\ CNA(M)\alpha+CNAD(M)\dot{\bar{\alpha}}+CNQ(M)\bar{q}\end{bmatrix}q_{din}S;$$

$$\begin{bmatrix}X_F\\ Y_F\\ Z_F\end{bmatrix}=\sum_{i=1}^{4}q_{din}S\begin{bmatrix}-CAd(M,\delta_i)\\ CYd(M,\delta_i)\sin\phi_i\\ -CNd(M,\delta_i)\cos\phi_i\end{bmatrix}\approx\sum_{i=1}^{4}q_{din}S\begin{bmatrix}-CAd(M,\delta_i)\\ CYD(M)\delta_i\sin\phi_i\\ -CND(M)\delta_i\cos\phi_i\end{bmatrix};$$

$$\begin{bmatrix} X_{TVC} \\ Y_{TVC} \\ Z_{TVC} \end{bmatrix} = \begin{bmatrix} (1-\mu_P)P \\ 0 \\ 0 \end{bmatrix} + \frac{1}{4}\sum_{i=1}^{4} P \begin{bmatrix} \mu_P \cos\delta_{TVCi} \\ \mu_P \sin\delta_{TVCi} \sin\phi_i \\ -\mu_P \sin\delta_{TVCi} \cos\phi_i \end{bmatrix} \approx \frac{1}{4}\sum_{i=1}^{4} P \begin{bmatrix} (1-\mu_P) + \mu_P \cos\delta_{TVCi} \\ \mu_P \delta_{TVCi} \sin\phi_i \\ -\mu_P \delta_{TVCi} \cos\phi_i \end{bmatrix};$$

Where α_s, α, β are the spatial angle of attack, angle of attack, and sideslip angle, respectively; q_{din}, S are the dynamic pressure and characteristic area, respectively; P, μ_P are the magnitude and coefficient of the thrust vector contributing to lateral motion.

The dimensionless components are determined as follows:

$$\bar{p} = p\frac{D}{2V};\ \bar{q} = q\frac{D}{2V};\ \bar{r} = r\frac{D}{2V};\ \dot{\bar{\alpha}} = \dot{\alpha}\frac{D}{2V}$$

The total external moments acting on the TLCT-3 are determined by the following expression:

$$\begin{bmatrix} L \\ M \\ N \end{bmatrix} = \begin{bmatrix} L_A \\ M_A \\ N_A \end{bmatrix} + \begin{bmatrix} L_F \\ M_F \\ N_F \end{bmatrix} + \begin{bmatrix} L_{TVC} \\ M_{TVC} \\ N_{TVC} \end{bmatrix} \quad (6)$$

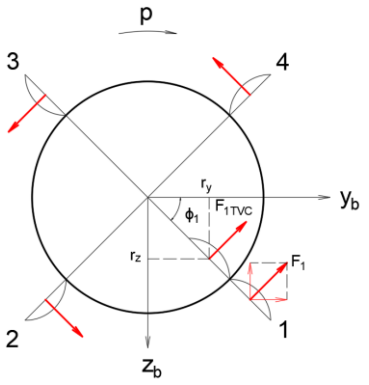

Figure 3. *Control force diagram in the fin plane.*

Where the components of the external moments are determined from the following expressions:

$$\begin{bmatrix} L_A \\ M_A \\ N_A \end{bmatrix} = \begin{bmatrix} CLL(M,\beta,p,r) \\ CM(M,\alpha,\dot{\alpha},q) \\ CLN(M,\beta,p,r) \end{bmatrix} q_{din}SD \approx \begin{bmatrix} CLLB(M)\beta + CLLP(M)\bar{p} + CLLR(M)\bar{r} \\ CMA(M)\alpha + CMAD(M)\dot{\bar{\alpha}} + CMQ(M)\bar{q} \\ CLNB(M)\beta + CLNP(M)\bar{p} + CLN(M)\bar{r} \end{bmatrix} q_{din}SD;$$

$$\begin{bmatrix} L_F \\ M_F \\ N_F \end{bmatrix} = \sum_{i=1}^{4} q_{din}SD \begin{bmatrix} CLLd(M,\delta_i) \\ CMd(M,\delta_i)\cos\phi_i \\ CLNd(M,\delta_i)\sin\phi_i \end{bmatrix} \approx \sum_{i=1}^{4} q_{din}SD \begin{bmatrix} CLLD(M)\delta_i \\ CMD(M)\delta_i \cos\phi_i \\ CLND(M)\delta_i \sin\phi_i \end{bmatrix};$$

$$\begin{bmatrix} L_{TVC} \\ M_{TVC} \\ N_{TVC} \end{bmatrix} = \sum_{i=1}^{4} \begin{bmatrix} 0 & -r_{zi} & r_{yi} \\ r_{zi} & 0 & -r_{xi} \\ -r_{yi} & r_{xi} & 0 \end{bmatrix} \begin{bmatrix} X_{TVCi} \\ Y_{TVCi} \\ Z_{TVCi} \end{bmatrix} \approx \sum_{i=1}^{4} \begin{bmatrix} -\frac{1}{4} r \mu_P P \delta_i \\ \frac{1}{4} r_x \mu_P P \delta_i \cos\phi_i \\ \frac{1}{4} r_x \mu_P P \delta_i \sin\phi_i \end{bmatrix};$$

Thus, the 6DOF model of the TLCT-3 has been established. The next task is to develop a control system model to construct the desired trajectory and simulate the controlled object tracking that desired trajectory.

2.2. Development of the control system model for the three-channel flight device

2.2.1. Command generation block model

The trajectory of the TLCT-3 in the default mode (top-attack) is shown in figure 4 [6].

The pre-guidance phase occurs before the cruise engine is activated. During this phase, the system ensures that the TLCT-3 reaches a safe separation distance after the launch motor operates. The 6DOF simulation model for this phase is implemented to determine the initial velocity parameters and Euler orientation angles for the subsequent phase.

The climb phase begins when the cruise engine is activated. During this phase, the TLCT-3 accelerates and ascends at a constant pitch angle until one of two limits is reached: an altitude of approximately 160 meters or the seeker's look angle (the angle between the line of sight (LOS) and the symmetric axis) approaches its maximum value. If the TLCT-3 reaches an altitude of 160 meters without hitting the look angle limit, it transitions to the altitude hold mode. In altitude hold mode, the TLCT-3 maintains altitude by generating a balanced angle of attack, α_{trim}, which ensures a level flight trajectory. As the TLCT-3 approaches the target in altitude hold mode, the seeker's look angle becomes increasingly negative. If this value exceeds the allowable limit (based on the maneuvering capability of the TLCT-3), the terminal guidance phase is activated. This phase adjusts the trajectory to maintain the look angle within limits and creates an appropriate impact angle with the target.

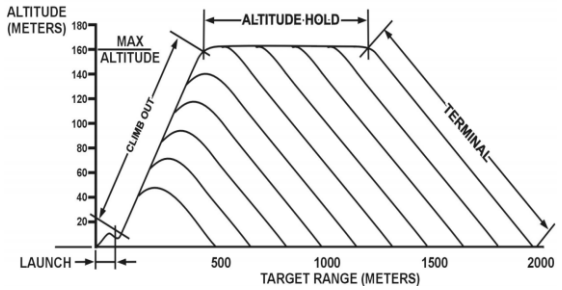

Figure 4. *Top attack flight path.*

The trajectory of the TLCT-3 in direct attack mode is shown in figure 5. In direct attack mode, the seeker's look angle limit is smaller compared to the top attack mode. Therefore, across the entire range, the look angle reaches its limit before the TLCT-3 attains its maximum altitude. Consequently, in this mode, a level flight trajectory does not occur.

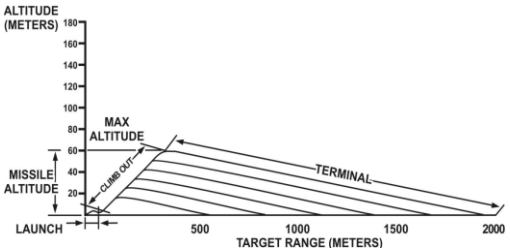

Figure 5. *Direct attack flight path.*

The yaw guidance law is designed similarly to the pitch channel in the terminal phase to ensure minimal miss distance at the intercept point. Meanwhile, the roll guidance law is analogous to the pitch channel in the initial phase, maintaining a fixed roll angle as required.

Thus, the guidance laws corresponding to each phase are constructed as follows [7]:

Flight phases		**Top attack mode**	**Direct attack mode**
Pitch channel	Climb	$u_p = \theta_{DES1} - \theta$	$u_p = \theta_{DES2} - \theta$
	Altitude Hold	$u_p = \alpha_{trim} - \theta$	-
	Terminal	$u_p = N\frac{d\varphi}{dt} + \frac{N}{2}\frac{V}{R}\left(\varphi - \varphi_{DES}\right)$	$u_p = N\frac{d\varphi}{dt}$
Yaw channel		$u_y = N\frac{d\chi}{dt}$	$u_y = N\frac{d\chi}{dt}$
Roll channel		$u_r = \phi_0 - \phi$	$u_r = \phi_0 - \phi$

Where θ_{DES} and α_{trim} are the desired pitch angle and the balanced angle of attack, respectively; φ, φ_{DES} and R are the look angle, desired look angle, and the missile-to-target distance, respectively; N is the navigation constant.

2.2.2. Autopilot block model

The TLCT-3 has a control system consisting of three independent channels: pitch, yaw, and roll. To decompose the missile's motion into components for each channel, the following assumptions are applied:

1) The TLCT-3 has a low flight ceiling (not exceeding 160 m), so the ambient temperature, air density, and gravitational acceleration can be considered constant throughout the flight, i.e.:

$$T = T_0; \quad \rho = \rho_0 = 1,225 kg/m^3; \quad g = g_0 = 9,80665 m/s^2 \tag{7}$$

2) The axial velocity of the missile is significantly greater than the lateral motion, i.e.:

$$v \ll u, \quad w \ll u, \quad u \approx V \tag{8}$$

3) The target has a low velocity (up to 75 km/h), so the maneuverability requirements for the TLCT-3 are not significant. This implies that the angles of attack and sideslip can be considered small, i.e.:

$$\alpha = \arctan\frac{w}{u} \approx \frac{w}{V}; \quad \beta = \arcsin\frac{v}{V} \approx \frac{v}{V}; \tag{9}$$

4) The TLCT-3 is controlled simultaneously across all three channels: roll, pitch, and yaw, where the roll channel is controlled to maintain the missile's initial roll angle state. This means that during the flight, the roll angle changes by a small value, i.e.:

$$p \approx 0; \quad \phi \approx \phi_0 = 0; \quad r \approx 0; \quad \psi \approx \psi_0 = 0 \tag{10}$$

5) Due to the small rotational velocity of the TLCT-3 around its center of mass, the effects of rotational motion in the pitch and yaw channels on the roll channel can be neglected. This means the aerodynamic force and moment components in the roll channel are:

$$X_A \approx X_A(M, \alpha_s); \quad L_A = L_A(M, \alpha_s, p) \tag{11}$$

6) The inclination angle component of the trajectory changes slowly over time, so around the point of interest θ_0, trigonometric functions can be considered nearly constant, i.e.:

$$\sin\theta \approx \sin\theta_0; \quad \cos\theta \approx \cos\theta_0 \tag{12}$$

7) The axial velocity component of the TLCT-3 changes over time, especially during the acceleration phase as the missile gains altitude. However, around the point of interest, where the error $\Delta V/V \leq 10\%$, this value can be considered constant, i.e.:

$$V = V_0; \quad M = M_0 = V_0 / a \tag{13}$$

Combined with the assumptions, from the three differential equations describing the motion of the center of mass of the TLCT-3 in the body-attached coordinate system $x_B y_B z_B$, we obtain:

$$\dot{v} = Y/m - rV_0; \; \dot{w} = Z/m - (pv - qu) \tag{14}$$

Where:

$$Y = Y_A + Y_F + Y_{TVC} + Y_G$$

$$\approx -\frac{CNA(M_0)q_{din}S}{V_0}v + \frac{CNQ(M_0)q_{din}SD}{2V_0}r + \left(CND(M_0)q_{din}S + \frac{1}{4}\mu_P P\right)\sum_{i=1}^{4}\delta_i \sin\phi_i$$

$$Z = Z_A + Z_F + Z_{TVC} + Z_G \approx -\frac{CNA(M_0)q_{din}S}{V_0}w + \frac{CNAD(M_0)q_{din}SD}{2V_0^2}\dot{w} + \frac{CNQ(M_0)q_{din}SD}{2V_0}q -$$

$$-\left(CND(M_0)q_{din}S + \frac{1}{4}\mu_P P\right)\sum_{i=1}^{4}\delta_i \cos\phi_i + mg\cos\theta_0$$

Expanding expression (14) yields expressions (15) and (16):

$$\dot{v} = Y^v v + Y^\delta \delta_y + Y^r r \tag{15}$$

Where

$$Y^{v} = -\frac{CNA(M_0)q_{din}S}{mV_0};\ Y^{\delta} = \frac{\left(CND(M_0)q_{din}S + \frac{1}{4}\mu_P P\right)}{m};$$

$$Y^{r} = \frac{CNQ(M_0)q_{din}SD}{2mV_0} - V_0;\ \delta_y = \sum_{i=1}^{4}\delta_i \sin\phi_i$$

$$Z^{\dot{w}}\dot{w} = Z^{w}w + Z^{\delta}\delta_p + Z^{q}q + g\cos\theta_0 \quad (16)$$

Where

$$Z^{\dot{w}} = 1 - \frac{CNAD(M_0)q_{din}SD}{2mV_0^2};\ Z^{w} = -\frac{CNA(M_0)q_{din}S}{mV_0};$$

$$Z^{\delta} = -\frac{\left(CND(M_0)q_{din}S + \frac{1}{4}\mu_P P\right)}{m};\ Z^{q} = \frac{CNQ(M_0)q_{din}SD}{2mV_0} + V_0;\ \delta_p = \sum_{i=1}^{4}\delta_i \cos\phi_i$$

Combined with the assumptions, from the three differential equations describing the rotational motion around the center of mass of the TLCT-3 in the body-attached coordinate system $x_B y_B z_B$, expression (17) is obtained.

$$\dot{p} \approx \frac{L}{I_{xx}};\qquad \dot{q} \approx \frac{M}{I_{yy}};\qquad \dot{r} \approx \frac{N}{I_{zz}} \quad (17)$$

Where

$$L = L_A + L_F + L_{TVC} = CLL(M_0)q_{din}SD + CLLP(M_0)q_{din}SD^2\frac{p}{2V_0} + \left(CLLD(M_0)q_{din}SD - \frac{1}{4}r\mu_P P\right)\sum_{i=1}^{4}\delta_i$$

$$M = M_A + M_F + M_{TVC} \approx \frac{CMA(M_0)q_{din}SD}{V_0}w + \frac{CMAD(M_0)q_{din}SD^2}{2V_0^2}\dot{w} + \frac{CMQ(M_0)q_{din}SD^2}{2V_0}q +$$

$$+\left(CMD(M_0)q_{din}SD + \frac{1}{4}r_x\mu_P P\right)\sum_{i=1}^{4}\delta_i\cos\phi_i$$

$$N = N_A + N_F + N_{TVC} \approx -\frac{CMA(M_0)q_{din}SD}{V_0}v + \frac{CMQ(M_0)q_{din}SD^2}{2V_0}r + \left(CMD(M_0)q_{din}SD + \frac{1}{4}r_x\mu_P P\right)\sum_{i=1}^{4}\delta_i\sin\phi_i$$

Expanding expression (17) yields expressions (18), (19), and (20).

$$\dot{p} \approx L^0 + L^p p + L^{\delta}\delta_r \quad (18)$$

Where

$$L^0 = \frac{CLL(M_0)q_{din}SD}{I_{xx}};\ L^p = \frac{CLLP(M_0)q_{din}SD^2}{2V_0 I_{xx}};\ L^{\delta} = \frac{\left(CLLD(M_0)q_{din}SD - \frac{1}{4}r\mu_P P\right)}{I_{xx}};\ \delta_r = \sum_{i=1}^{4}\delta_i$$

$$\dot{q} \approx M^{w}w + M^{\dot{w}}\dot{w} + M^{q}q + M^{\delta}\delta_p \quad (19)$$

Where

$$M^{w} = \frac{CMA(M_0)q_{din}SD}{V_0 I_{zz}};\ M^{\dot{w}} = \frac{CMAD(M_0)q_{din}SD^2}{2V_0^2 I_{zz}};\ M^{q} = \frac{CMQ(M_0)q_{din}SD^2}{2V_0 I_{zz}};$$

$$M^{\delta} = \frac{\left(CMD(M_0)q_{din}SD + \frac{1}{4}r_x\mu_P P\right)}{I_{zz}}$$

$$\dot{r} \approx N^{v}v + N^{r}r + N^{\delta}\delta_{y} \tag{20}$$

Where

$$N^{v} = -\frac{CMA(M_0)q_{din}SD}{V_0 I_{yy}};\ N^{r} = \frac{CMQ(M_0)q_{din}SD^2}{2V_0 I_{yy}};\ N^{\delta} = \frac{\left(CMD(M_0)q_{din}SD + \frac{1}{4}r_x\mu_P P\right)}{I_{yy}}$$

Combined with the assumptions, from the three differential equations describing the rotational motion around the center of mass of the TLCT-3 in the ground coordinate system $x_E y_E z_E$, expression (21) is obtained.

$$\dot{\phi} \approx p;\qquad \dot{\theta} = q;\qquad \dot{\psi}\cos\theta_0 = r; \tag{21}$$

From the transformations of the flight dynamics model of the TLCT-3 combined with the assumption conditions, a system of differential equations describing the independent motion of each control channel is obtained:

- Motion in the roll channel:

$$\begin{cases} \dot{p} \approx L^{p}p + L^{\delta}\delta_{r} \\ \dot{\phi} \approx p \end{cases} \tag{22}$$

- Motion in the pitch channel:

$$\begin{cases} Z^{\dot{w}}\dot{w} = Z^{w}w + Z^{\delta}\delta_{p} + Z^{q}q + g\cos\theta_0 \\ \dot{q} \approx M^{w}w + M^{\dot{w}}\dot{w} + M^{q}q + M^{\delta}\delta_{p} \\ \dot{\theta} = q \end{cases} \tag{23}$$

- Motion in the yaw channel:

$$\begin{bmatrix} \dot{\psi}\cos\theta_0 \\ \dot{r} \\ \dot{v} \end{bmatrix} = \begin{bmatrix} 0 & 1 & 0 \\ 0 & N^{r} & N^{v} \\ 0 & Y^{r} & Y^{v} \end{bmatrix} \begin{bmatrix} \psi \\ r \\ v \end{bmatrix} + \begin{bmatrix} 0 \\ N^{\delta} \\ Y^{\delta} \end{bmatrix} \delta_{y} \tag{24}$$

The autopilot structure of the TLCT-3 is built based on the classical PID controller, which is simple and effective. The structure of the pitch channel controller includes an angle tracking controller and a line-of-sight angular velocity tracking controller. The yaw channel uses a line-of-sight angular velocity tracking controller, while the roll channel employs a roll angle stabilization controller. The parameters of the corresponding PID controllers are determined using the step response optimization tool in Matlab/Simulink.

3. SIMULATION, CALCULATION, AND DISCUSSION

3.1. Input Data

To support simulation, verification, and evaluation of results, the following data are used as input parameters for the program:

1) Characteristic data of TLCT-3

TimeTable = [0.0 0.3 0.6 1.2 1.8 2.4 4.2 5.2];

P_Table = [0.0 570 650 750 770 650 50 0.0];

m_Table = [11.25 11.16 11.06 10.82 10.58 10.38 10.16 10.15];

CG_Table = [0.565 0.555 0.544 0.519 0.493 0.471 0.447 0.446];

Ixx_Table = [0.0252 0.0250 0.0248 0.0244 0.0239 0.0235 0.0231 0.0231];

Iyy_Table = [0.985 0.979 0.973 0.958 0.942 0.929 0.915 0.914];

The aerodynamic coefficients are calculated and directly obtained from the Missile Datcom software.

2) Command generation block:

$\theta_{DES1} = 30^0$; $\theta_{DES2} = 22^0$; $\alpha_{trim} = 2^0$; $\varphi_{DES} = 45^0$.

3.2. Methods and simulation tools

The Matlab/Simulink software is used to build the simulation program for the TLCT-3 control loop based on the designed models. Simulations are conducted, and results are analyzed and evaluated under two tactical scenarios: top attack and direct attack modes of the TLCT-3 (figure 6).

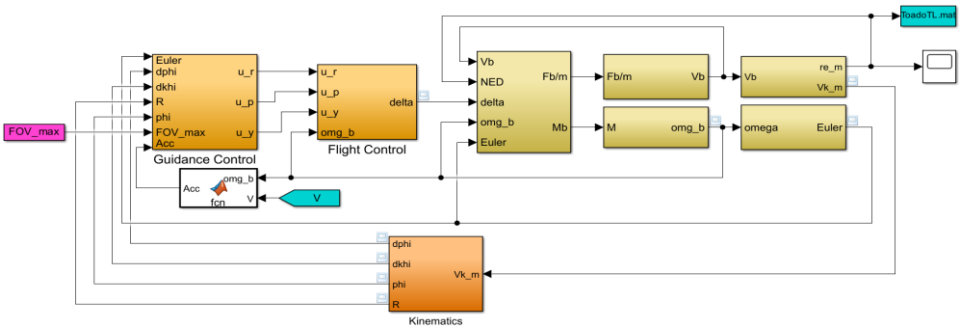

Figure 6. *TLCT-3 Simulation Program Interface.*

3.3. Simulation results and discussion

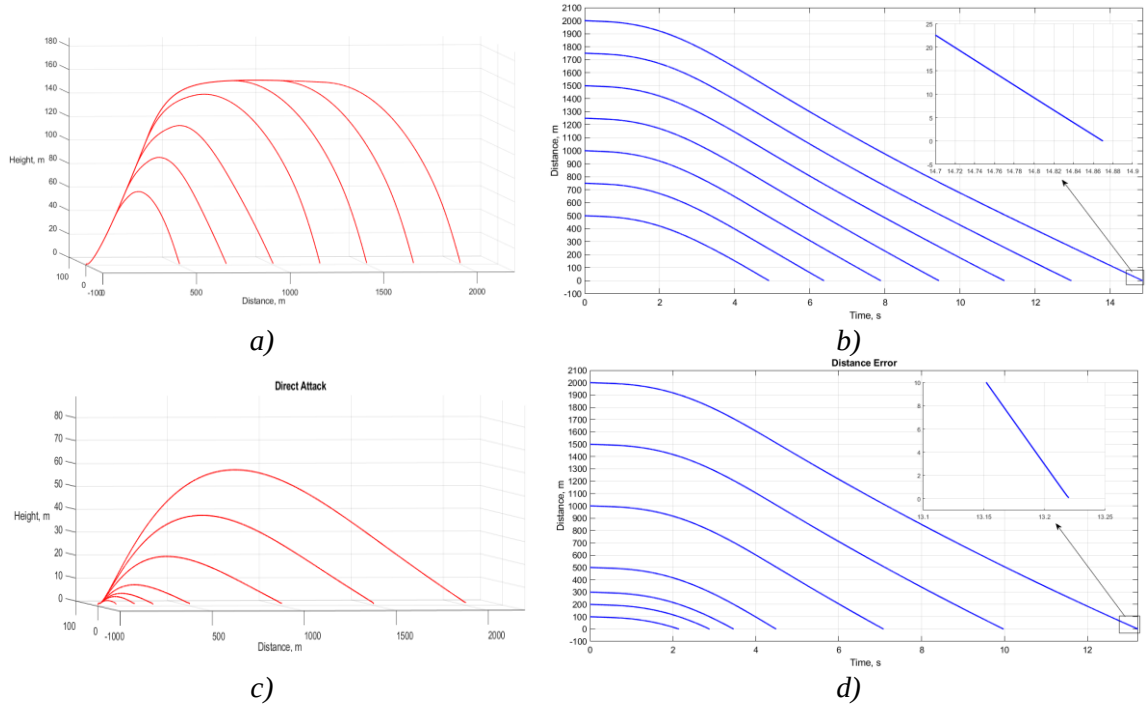

a) *b)*

c) *d)*

Figure 7. *Simulation results in different attack modes:*
a) Top attack trajectory; b) Miss distance in top attack mode;
c) Direct attack trajectory; d) Miss distance in direct attack mode.

The simulation results corresponding to the range from 500 to 2000 meters for the top attack mode and from 100 to 2000 meters for the direct attack mode are shown in figures 7a-7d.

Comments:

The miss distance across the entire range of the TLCT-3, in both top attack mode (500–2000 m) and direct attack mode (100–2000 m), is very small (≤ 0.2 m), confirming the accuracy of the control system model. In direct attack mode, due to the smaller field-of-view limit, there is no level-flight phase, and the missile transitions directly to the terminal guidance phase, with a maximum altitude of approximately 60 m, consistent with the actual data of the Javelin-type TLCT-3. In top attack mode, with a larger field-of-view limit, level-flight occurs at longer ranges before transitioning to the terminal guidance phase. However, at shorter ranges, the TLCT-3 transitions directly to the terminal guidance phase without a level-flight phase. The maximum altitude in this mode is approximately 160 m, which also aligns with actual data. The simulation results are consistent with real-world data, providing a solid theoretical foundation for designing the control system for the TLCT-3. This is the first study to provide comprehensive simulation results for all tactical scenarios across the entire range of the Javelin-type TLCT-3.

4. CONCLUSIONS

Based on the study of the Javelin-type three-channel flight device, the authors calculated its characteristics, developed a flight dynamics model, and synthesized the control system, including the command generation block and the autopilot block, according to tactical scenarios. Subsequently, simulations were conducted to compare and evaluate the effectiveness of these models.

The simulation results successfully closed the 6DOF control loop of the TLCT-3 and examined the entire range of operation in both top attack and direct attack modes. This is a novel contribution compared to previous studies and provides a foundation for designing the TLCT-3 control system. However, the paper focuses on constructing the control system based on classical control theory. With advancements in science and technology, it is entirely feasible to apply modern control theory and intelligent control techniques to enhance the quality of the control system. This issue will be considered in the authors' future publications.

REFERENCES

[1]. A. B. Рябцев, "*Оценка перспектив развития современных образцов зарубежных противотанковых ракетных комплексов*," "Молодой учёный", № 48 (390), (2021).

[2]. Marko Radovanović *et al*, "*Analysis Of The Development Of Five Generation Of Anti-Armor Missile Systems*," J. Scientific Technical Review, Vol.73, No. 1, pp. 26-37, (2023).

[3]. T. V. Hai *et al.*, "*Synthesis of Suboptimal Guidance Law for Anti-Tank Guided Missile with Terminal Impact Angle Constraint Based on the SDRE Technique,*" Archives of Advanced Engineering Science, Vol. 00, pp. 1-7, (2023).

[4]. T. V. Hai *et al.*, "*Nonlinear Guidance Laws for Anti-tank Guided Missile to Intercept Maneuvering Tank Targets Using Optimal Error Dynamics and Relative Virtual Model,*", J. Aerosp. Technol. Manag., v16, e2424, (2024).

[5]. Harris *et al.*, "*Performance of a Fire-and-Forget Anti-Tank Missile with a Damaged Wing*". Faculty Publications - Biomedical, Mechanical, and Civil Engineering. 7, (2009).

[6]. Headquarters, Department of the Army, "*Javelin - Close Combat Missile System, Medium*", TC 3-22.37, (2013).

[7]. Paul Zarchan, "*Tactical and Strategic Missile Guidance*," American Institute of Aeronautics and Astronautics, Inc., pp. 569-601, (2012).

TÓM TẮT

Mô phỏng vòng điều khiển chuyển động 6DOF của thiết bị bay ba kênh

Bài báo trình bày phương pháp xây dựng hệ thống điều khiển và mô phỏng vòng điều khiển kín chuyển động 6 bậc tự do (6DOF) của thiết bị bay ba kênh kiểu Javelin (TLCT-3). Dựa trên các dữ liệu công bố về tính năng chiến kỹ thuật của TLCT-3, nhóm tác giả đã phân tích, tính toán đặc trưng hình học, quán tính, khí động để làm dữ liệu đầu vào của đối tượng điều khiển cho chương trình mô phỏng. Đồng thời, nhóm nghiên cứu đã xây dựng mô hình khối tạo lệnh điều khiển, khối tự động lái và đối tượng điều khiển để thiết kế chương trình mô phỏng. Kết quả mô phỏng theo hai kịch bản ***tấn công đột nóc*** *và* ***tấn công trực diện*** *khẳng định tính chính xác của các mô hình và sự phù hợp với tính năng chiến kỹ thuật của TLCT-3.*

Từ khoá: Thiết bị bay ba kênh; Mô phỏng vòng điều khiển; Chuyển động 6DOF.